International Journal of High-Rise Buildings
March 2018, Vol 7, No 1, 17-32
https://doi.org/10.21022/IJHRB.2018.7.1.17

International Journal of
High-Rise Buildings
www.ctbuh-korea.org/ijhrb/index.php

# Embossed Structural Skin for Tall Buildings

**Jin Young Song[1†], Donghun Lee[2], James Erickson[3], Jianming Hao[4], Teng Wu[4], and Bonghwan Kim[5]**

[1]*Department of Architecture, University at Buffalo, The State University of New York*
[2]*Leslie E. Robertson Associates*
[3]*Arizona State University*
[4]*Department of Civil, Structural and Environmental Engineering, University at Buffalo, The State University of New York*
[5]*Skidmore, Owings & Merrill LLP*

**Abstract**

This paper explores the function of a structural skin with an embossed surface applicable to use for tall building structures. The major diagrid system with a secondary embossed surface structure provides an enhanced perimeter structural system by increasing tube section areas and reduces aerodynamic loads by disorienting major organized structure of winds. A parametric study used to investigate an optimized configuration of the embossed structure revealed that the embossed structure has a structural advantage in stiffening the structure, reducing lateral drift to 90% compared to a non-embossed diagrid baseline model, and results of wind load analysis using computational fluid dynamics, demonstrated the proposed embossed system can reduce. The resulting undulating embossed skin geometry presents both opportunities for incorporating versatile interior environments as well as unique challenges for daylighting and thermal control of the envelope. Solar and thermal control requires multiple daylighting solutions to address each local façade surface condition in order to reduce energy loads and meet occupant comfort standards. These findings illustrate that although more complex in geometry, architects and engineers can produce tall buildings that have less impact on our environment by utilizing structural forms that reduce structural steel needed for stiffening, thus reducing embodied $CO^2$, while positively affecting indoor quality and energy performance, all possible while creating a unique urban iconography derived from the performance of building skin.

**Keywords:** Structural skin, Diagrid system, Tall buildings, Façade, Wind computational fluid dynamics

## 1. Introduction: Thickness of Building Envelope

It has been more than 100 years since Le Corbusier designed the Dom-Ino system, an open floor plan prototype which signalled the liberation of architecture from the burden of exclusively designing structures with load bearing skins. This 'free façade' capable of hanging non-structural material to the envelope has become the standard of the building industry in the 21st century. The market driven culture and supply chain to the building industry has become highly sophisticated in the production of these curtain wall related systems. The transparency of non-load bearing skin systems fuelled by a universal culture of modernism has become the exclusive building system for buildings that now dominate the skyline of all major global cities. However, the resulting decreased thermal mass in the production and on-site application of aluminium curtainwall systems, and societies growing concern for reducing the building industries impact on the environment, has contributed to the development of products to be added to curtainwall systems rather a rethinking of the tall building system as a whole. Increasingly stringent minimum efficiency energy standards call for improved thermal performance of the building envelope as well as solar controls, however the standardization of solutions results in a common architectural response to a climate, building type, and orientation. Often, when budgets cannot accommodate high performance glazing or external shading systems across these large façades, the window to wall ratio is often adjusted making for the right U-factor for meeting local codes. In contrast to the standardization of solutions, digital design and fabrication tools, and advances in material research are contributing to the "return of ornaments" in the building skin, argued to be the new type of subjectivity characteristics of the digital age (Picon, 2014).

An increasing amount of opaque area in the envelope, due in part to energy efficiency requirements and in part to address the collective meaning of our digital culture (Picon, 2014), is an opportunity to re-evaluate the integration of structure and skin relationship in the context of contemporary cultural and sustainability values, and the current state-of-the-art technology. It is with this as a

†Corresponding author: Jin Young Song
Tel: +1-716-829-5898
E-mail: jsong11@buffalo.edu

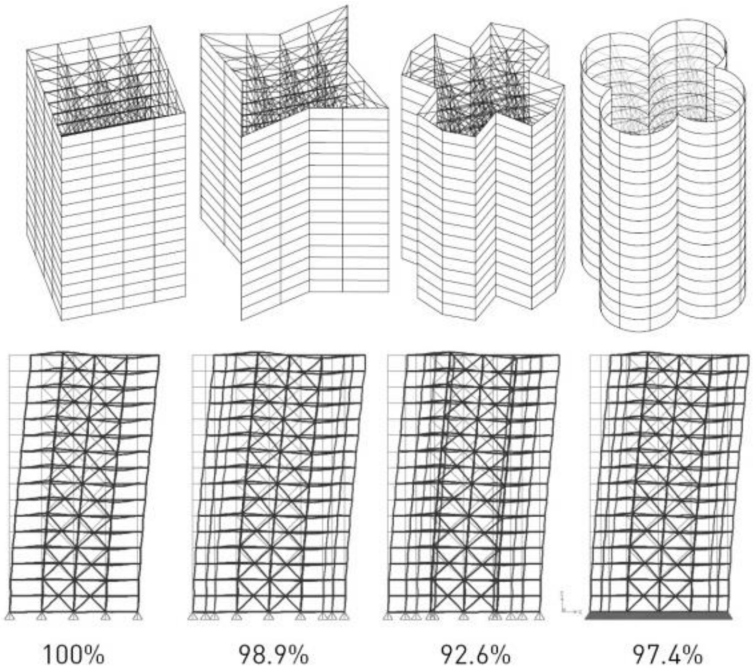



**Figure 1.** Surface Shape and Structural Stiffness based on Same GFA (Structural analysis by SAP2000, Computer and Structures, 2017).

foundation that the research takes off, exploring an embossed skin system as a novel way to integrate skin and structure.

A structural analysis and parametric studies are used to demonstrate the performance of the embossed skin form with additional structural benefits illustrated through computational fluid dynamics (CFD) analysis allows for reduced structural material and improved resiliency from lateral loads. The resulting form is evaluated for energy and daylighting performance, considering potential occupant thermal and visual comfort as well as the impact on the environment due to reduced embodied energy from the embossed structure.

## 2. Background: Structural Skin

To develop the increasing need for opaque envelope area in the building envelop, Neary (2017) studied envelope details by replacing conventional aluminium mullions with hybrid mullions of steel and aluminium cassette frames and explored options to stiffen the spandrel area by adding steel plates or rods. The result showed that the skin components have structural capacity to limit lateral drift and to reduce the primary steel frame tonnage. Additionally, it reduced the aluminium tonnage replacing the conventional curtain wall, which means reduced embodied $CO^2$ in construction materials. Based on this increased structural capability of the skin using the same area of conventional curtain wall system, more aggressive methods to integrate the primary building structure with envelope structure are explored: 'diagrid' and 'shape factor'. The diagrid structure is an efficient tubular system, consisting of brace frames as a main lateral force resisting system by overcoming the concerns of lateral stiffness and shear lag problem, which results in a reduction of the tonnage of primary structure compared to conventional moment frame systems. In recent years, it has received increasing attention and several iconic buildings are built with the system including, for example, the Hearst tower which used 20% less steel than conventionally framed structures (Rahimian et al., 2006). Research examining the diagrid system by Moon et al. (2007), an angle of diagrid bracing was optimized to find the most efficient diagrid configuration in a limit of lateral drift ratio of H/500. On top of the learning from this proven research, there are specific shapes factor affecting the overall stiffness. Fig. 1 shows conceptual tower modules with same gross floor area (GFA), presenting the structural benefit of the shape factor. The economic balance among workable lease span, increased façade construction area and construction details need to be considered but, the stiffness of tower design can be achieved from the skin shape. Therefore, the embossed surface is studied as a way of integration between diagrid and stiffness achieved from the skin shape.

For analysis, two models were used to compare the performance of the proposed embossed form. The baseline model is a parallelogram with the foot print measuring 54 m (x-axis) by 66.9 m (y-axis) with inside angles of 110° and 70°, 3409.5 $m^2$ per floor and GFA of 211,388 $m^2$, with

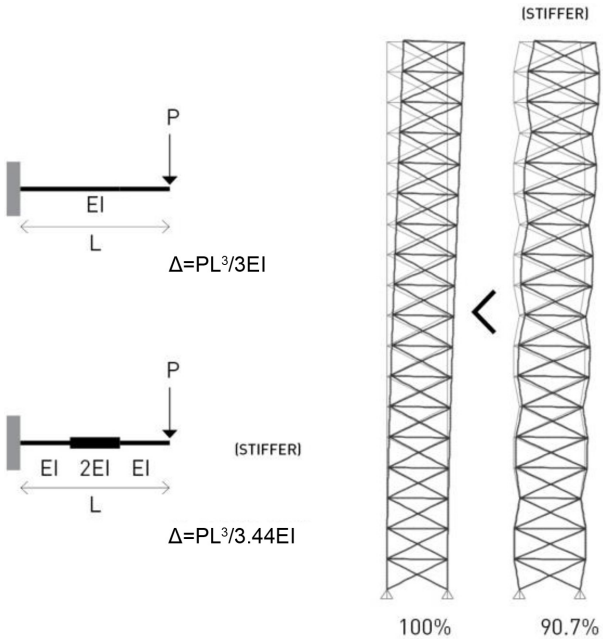



**Figure 2.** Beam Deflection Theory and Stiffness Increase in Building Structure.

the core service areas of both forms equal in area, shape, and volume. Derived from this baseline form, the embossed form averages 3396 $m^2$ per floor, varying between 3344.5 $m^2$ and 3527.5 $m^2$ for the largest floors. Both towers are 62 floors totalling 248 m in height. External envelope surface area, excluding the roof, is 60006.5 $m^2$ for the baseline and 67101 $m^2$ for the undulating surface that is the embossed form. Total volume of the baseline is 845553 $m^3$ and 845248 $m^3$ for the embossed. The models are rotated 30° from true north for energy analysis.

## 3. Embossed Structural Skin

The embossed skin is inspired by well-known practice of structure engineering: deflection of beam, diagrid system, and intrinsic stiffness of the shape. For a holistic integration of these principles, the surface shape features arch modules, which provide a structural benefit and enlarge the floor area. Given the same ground floor support, the emboss module provides an evident flexural rigidity by stiffening part of the cantilever, as conceptually described in Fig. 2. Having increased moment of inertia in the middle segment, the embossed surface structure provides increased lateral stiffness compared to a non-embossed, flat surface. In order to understand the behaviour of the emboss module, a simple parametric model is designed. Figs. 3 and 4 shows the process used to investigate optimal degrees of an appropriate number of embossed modules (aspect ratio), showing that the reduction is significant in approximately at 10 degree and the effect is insignificant in a model with more than five modules. Note the parametric study in Figs. 3 and 4 was conducted using a 2D model with a specified column span within a bay, allowing for the result to be adapted in 3D models with various column spans in a variety of bay widths.

In order to introduce the embossed skin to the tower, the diagrid system could be a solid solution not only in integrating the irregular embossed units into the 60-story building in a regular manner, but in transferring axial forces of each emboss unit to the main diagonal members. Specifically, the diagrid system enhances the lateral stiffness in the force-parallel direction. To test the structural efficiency of the embossed module suggested in Figs. 3 and 4, two three dimensional prototypes were simulated with different embossed angle and aspect ratios (Fig. 5). The baseline module with diagrid has 4 structural bays with 30’ span (120 ft × 120 ft). The emboss module has an identical condition to the baseline model except the center of the diagrid surfaces are embossed.

The same wind loads were applied to the center of the geometry of each floor and both have the same member sizes. As a result, 10 degree of embossing and 1:8 ratio showed the least roof drift by about 10%. As presented in the inter-story drift graph (Fig. 5), the embossed floors with the largest area (4th, 8th, 12th floors, etc.) showed the best drift-reduction effect, which also confirms the result shown in Fig. 4, the structural efficiency of the embossed form.

From these findings, the theoretical Emboss Tower is envisioned to offer many spatial benefits that are unique to the tower due to the innovative structural system (Figs. 6, 7, 8 and 9). While a typical moment frame construction with conventional curtain wall system could offer unobstructed views and ample daylight, the embossed form is

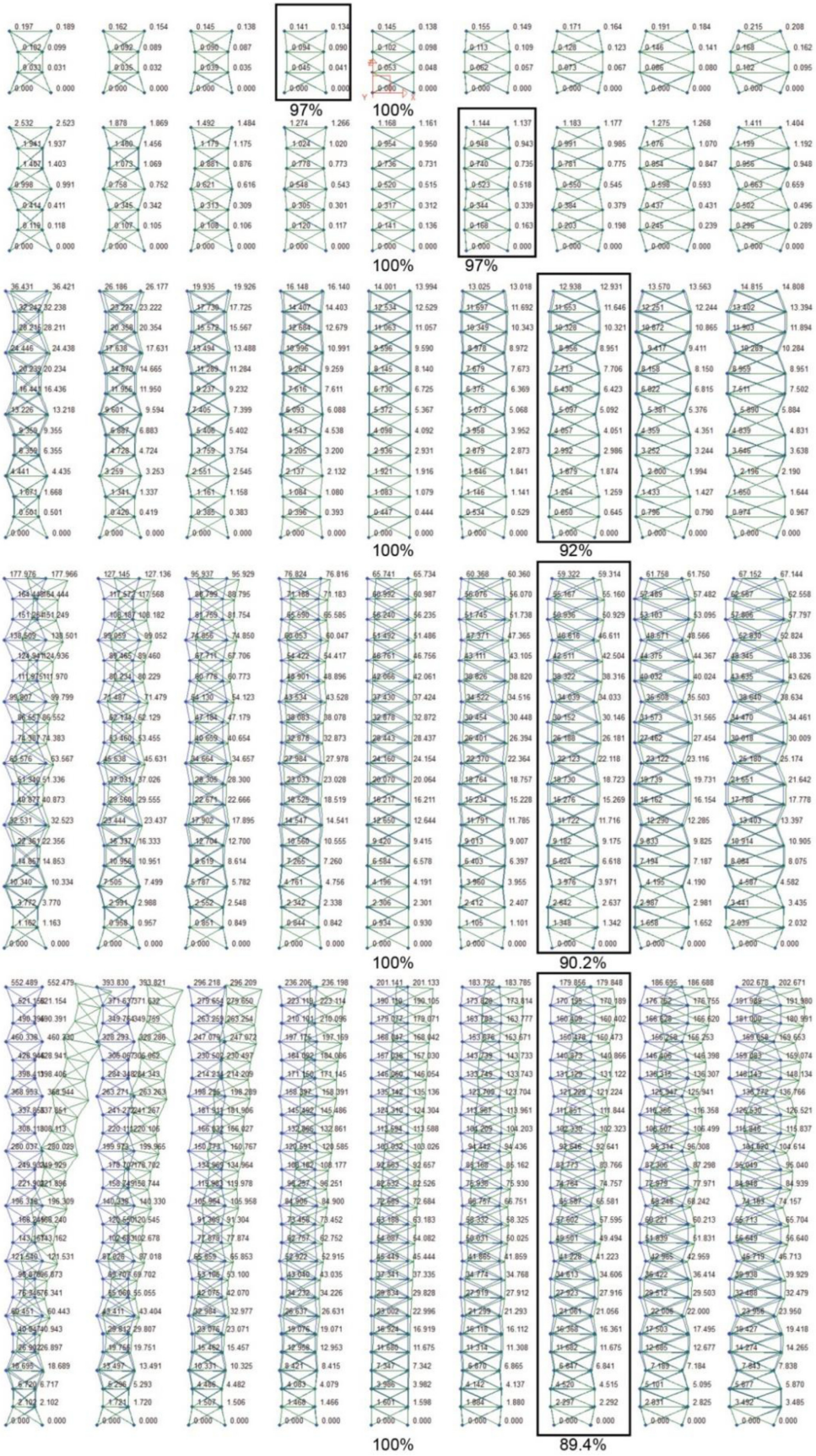



**Figure 3.** Surface Shape and Structural Stiffness.

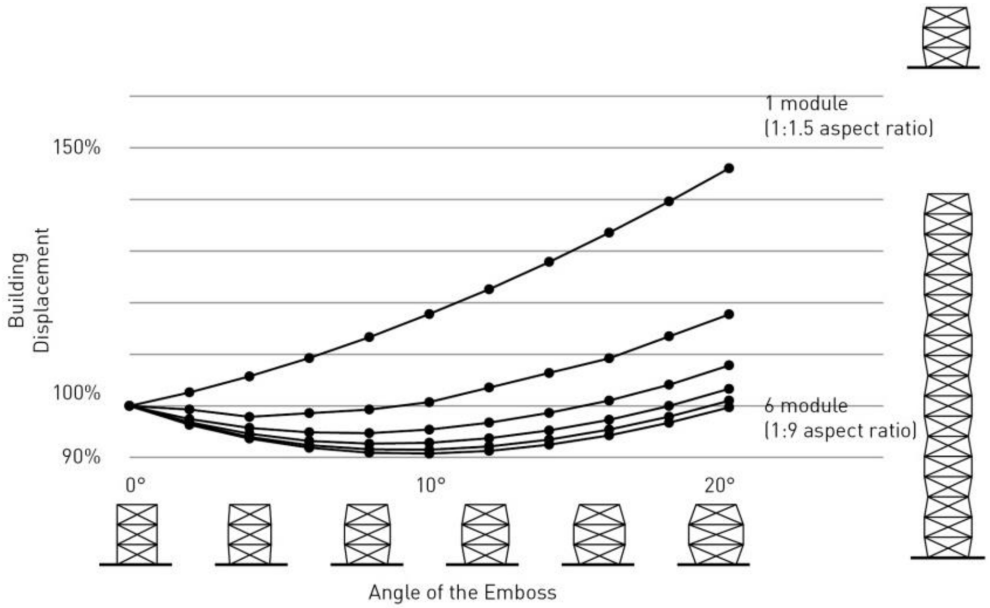



**Figure 4.** Building Displacement versus Emboss Angle and Aspect Ratio Relationship.

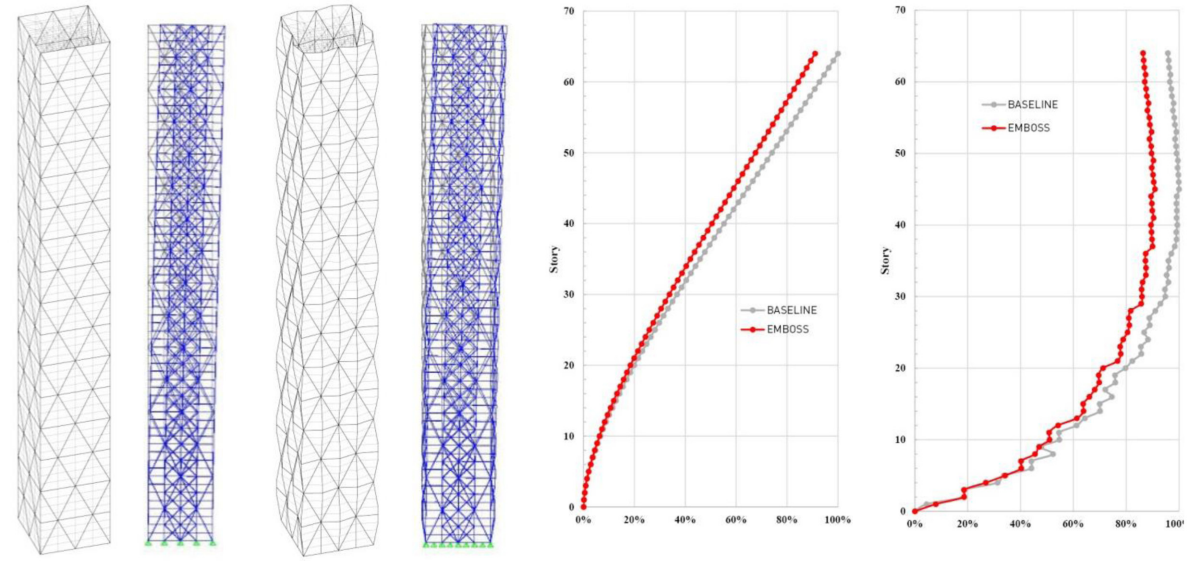



**Figure 5.** Increased Efficiency of Stacked Embossed Module: (a) and (b) have same area on the ground floor, same structural grid. (b) has more GFA than (a) due to the embossed skin. (c) Normalized cumulative story drift with respect to the maximum story drift. (d) Normalized inter-story drift with respect to the maximum inter-story drift.

envisioned to provide a more dynamic and flexible interior space due in part to the bay structures and bowed window walls.

## 4. Emboss for Wind Load Reduction

The wind induced performance on the emboss tower were examined numerically based on the computational fluid dynamics (CFD) approach (Blocken, 2014; Murakami, 1990; Murakami and Mochida, 1999; Tamura et al., 1997). In this study, both the full-scale simulation of the embossed tower and baseline models were simulated using commercial CFD software for comparison. The CFD computational domain covers 30×D, where D is the width of



**Figure 6.** Emboss Tower Rendering.

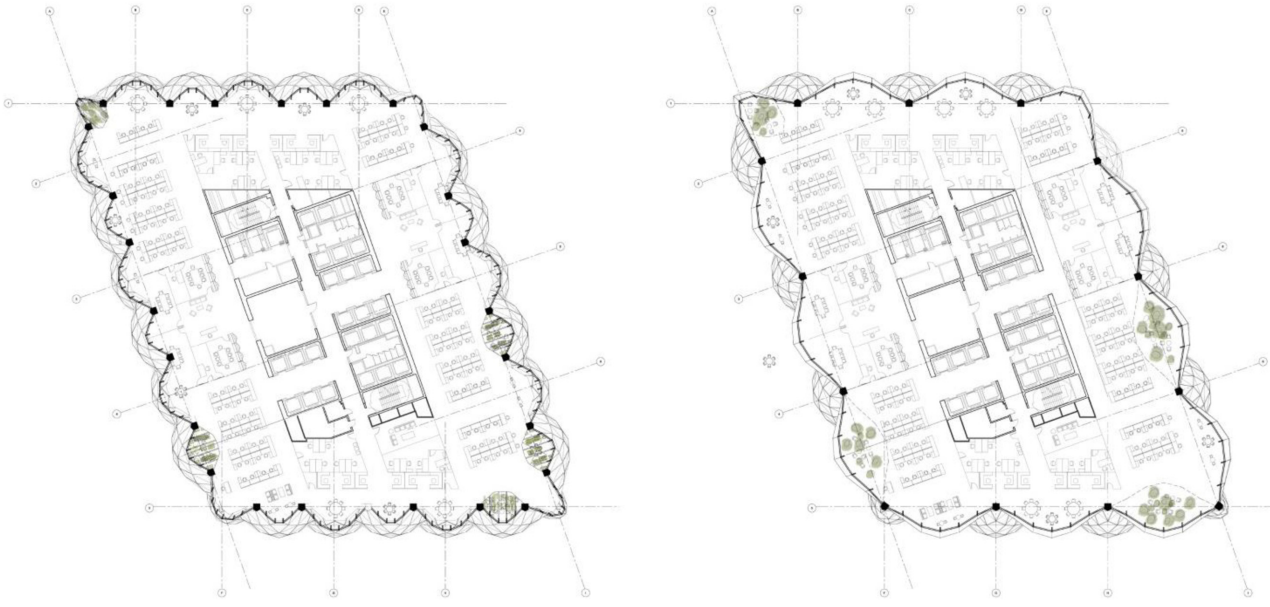


**Figure 7.** Emboss Tower Typical Plan.

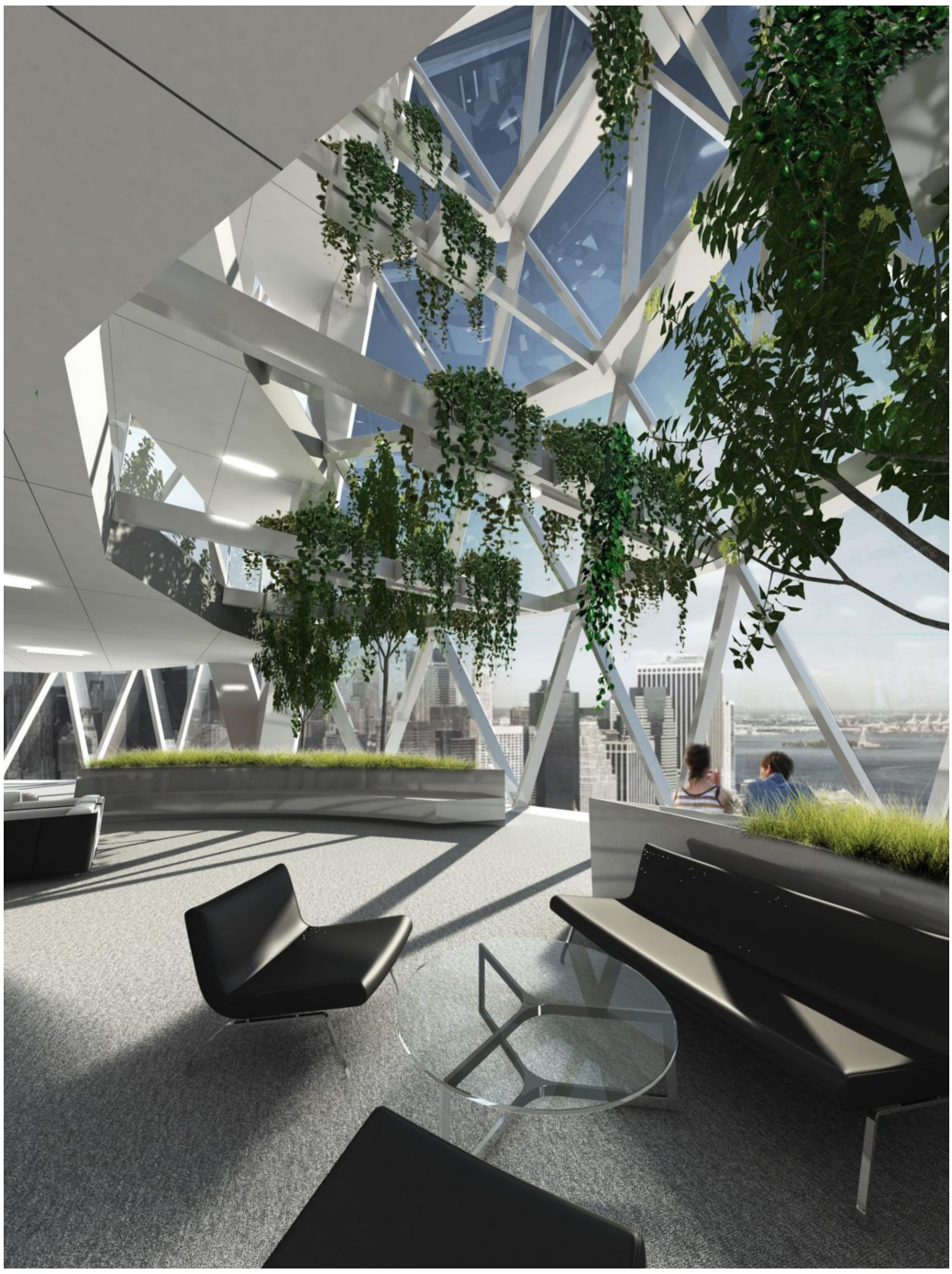


**Figure 8.** Atrium space in the Embossed surface.

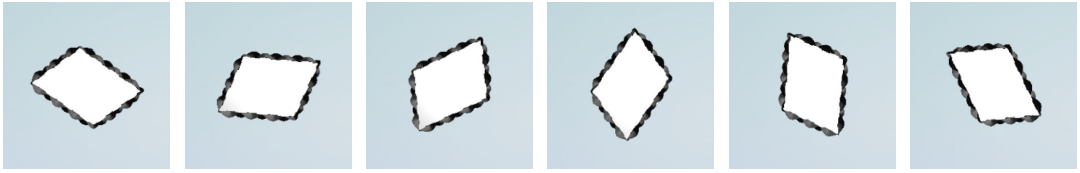
the building base, in the stream-wise direction, 15×D in the lateral direction, and 2×H, where H is the height of the building, in the vertical direction. Six different angles of attack were examined to investigate the performance under different wind directions, as shown in Table 1. The base shear force, one of the significant parameters to examine the total lateral wind load on the structure, was normalized by the baseline model results and summarized in the table.

Comparison of the normalized base shear forces varying with different angles of attack for each skin type are illustrated in Fig. 10. The results show that the embossed skin could significantly reduce the base shear force of the structure. For example, the base shear forces of the embossed skin type under 90° and 120° angles of attack are, respectively, 18.06% and 21.20% less than those of baseline model. The embossed skin type may facilitate the breakdown of the large-scale flow structures surrounding



**Figure 9.** Emboss Tower Sections.

**Table 1.** The normalized base shear forces subject to different angles of attack

| | Angle of attack (°) | | | | | |
|---|---|---|---|---|---|---|
| | 0° | 30° | 60° | 90° | 120° | 150° |
| Wind → |  | | | | | |
| | Normalized base shear forces | | | | | |
| Baseline | 100% | 100% | 100% | 100% | 100% | 100% |
| Emboss | 99.91% | 97.88% | 96.81% | 81.94% | 78.80% | 90.66% |
| Diff. | 0.09% | 2.12% | 3.19% | 18.06% | 21.20% | 9.34% |

Note: Wind direction is from left to right, and the wind speed is 135 ft/s

the tower. This results in partially-correlated smaller eddies, and hence reduces the wind loads on the tower. A similar effect can be observed with golf balls where small dimples arrayed across the surface can enable the ball to travel further than a perfectly smooth sphere. Figs. 11 and 12 show the velocity and pressure contours of the field under 0° angle of attack for each skin type. According to the figure, the wake flow generated by the embossed skin tower is much narrower than that of baseline type, which indicates a further reduction of wind effects.

## 5. Emboss for Reduced Embodied Energy

Embodied energy is the total amount of energy consumed from extraction to fabrication and measured here by the amount of carbon ($CO_2$) produced by a materials manufacturing process, which contributes to global climate change. Embodied energy can be mitigated by reducing the amount of steel required for a building. With the increased stiffness afforded to the emboss form, the steel tonnage could be reduced by 11000 tonnes or 35% less com-

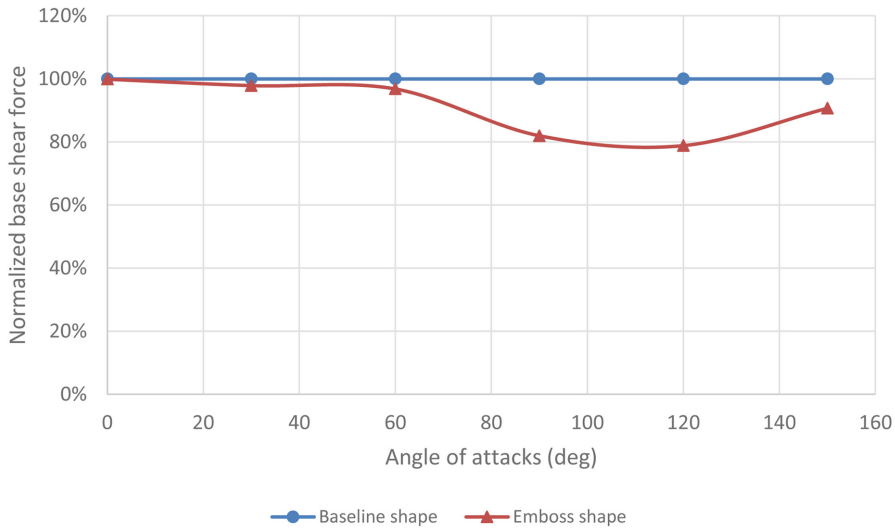
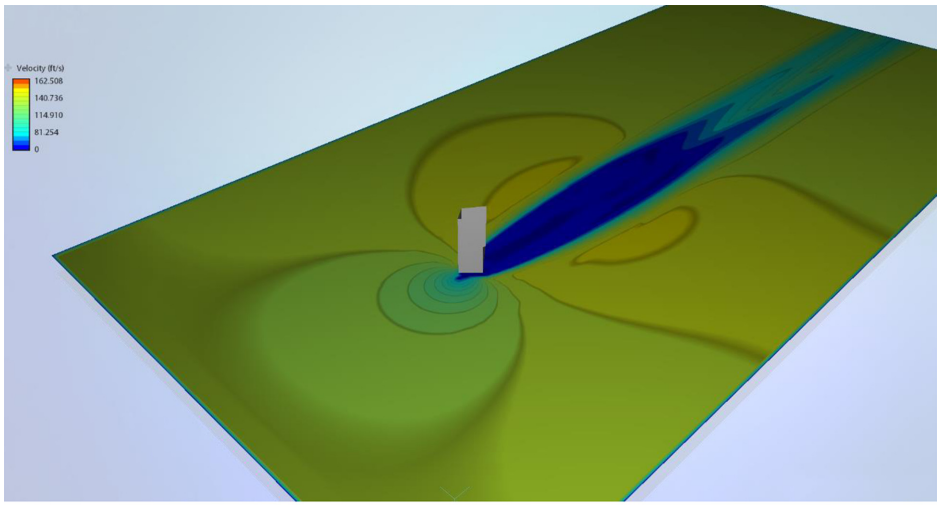
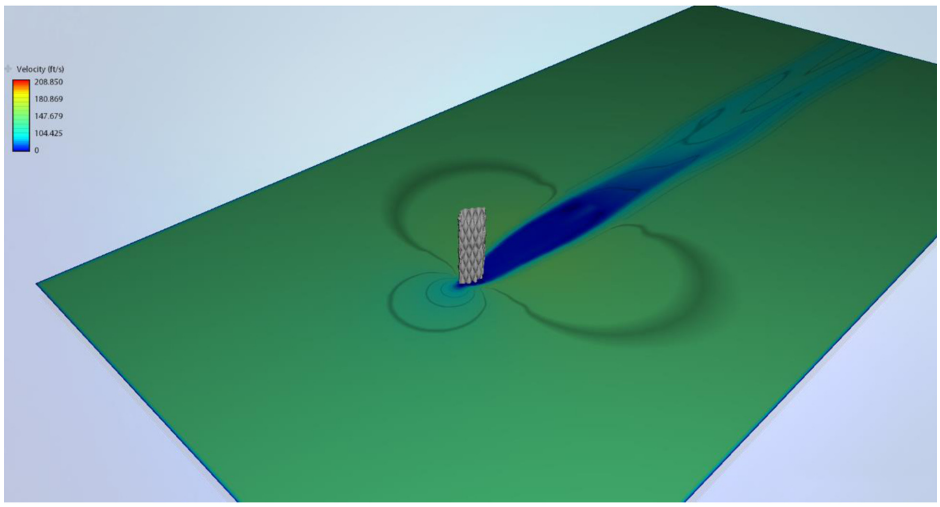



**Figure 10.** The comparison of the normalized base shear force for two skin types.

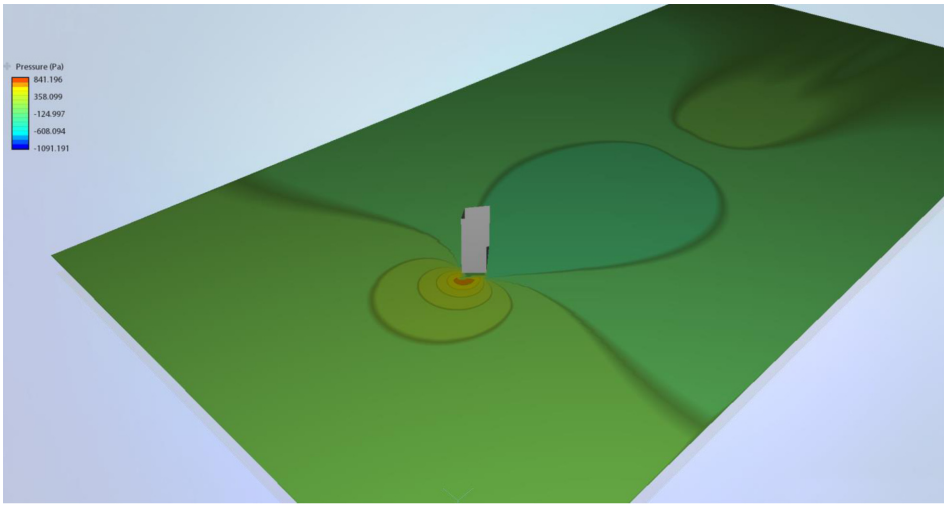



(a) Baseline Skin Type

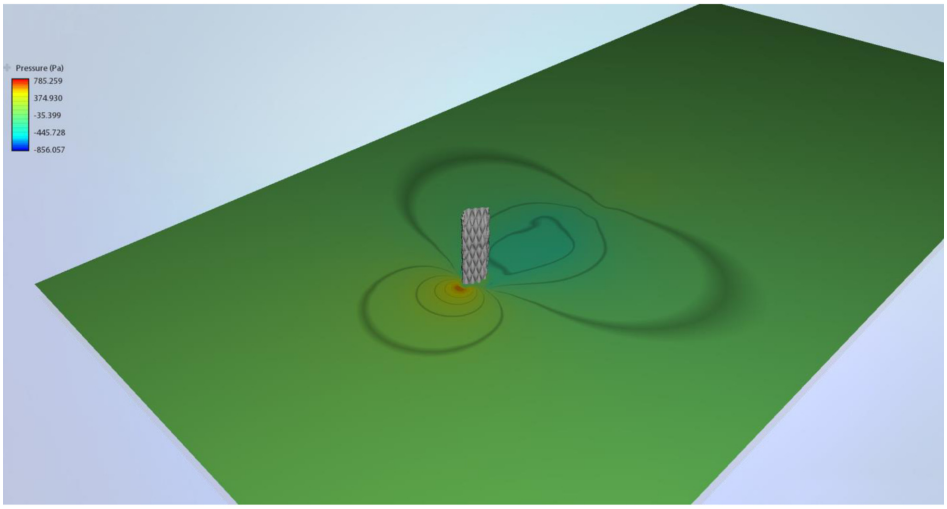



(b) Embossed Skin Type

**Figure 11.** Contour of Velocity Field of CFD Analysis for (a) Baseline Skin Type and (b) Embossed Skin Type.




(a) Baseline Skin Type




(b) Embossed Skin Type

**Figure 12.** Contour of Pressure Field of CFD Analysis for (a) Baseline Skin Type and (b) Embossed Skin Type.

pared to the base model. The steel tonnage was calculated based on structural member design, which was determined to meet the structural demands for (a) serviceability against wind load in equation H/500 and (b) strength design for the governing load combination of dead load, live load, and wind load in equation 1 per standard ASCE 7 (2010).

Equation 1:

$$1.2D+W+L$$

Wind load was estimated assuming the towers are located within the urban area of Manhattan, New York where the basic wind speed is assumed to be 123 mph. The Baseline tower was designed using moment frame system consisting of a braced core, moment resisting frame in perimeter and horizontal members connecting the core frame to the perimeter in moment connection. The Emboss tower was modelled using a core frame without bracing, the diagrid and emboss skin around the perimeter and horizontal members connecting the core frame to the perimeter in shear connection. For both models, all nodes in each story were constrained using a rigid diaphragm. All structural members were modelled with steel material.

Table 2 shows the results of the structural member design in terms of steel tonnage used in perimeter, core, and horizontal frames. In the table, the total steel tonnage used in the emboss model is about 64% of that used in the baseline model, which reveals that the emboss model has a significant benefit in transferring lateral forces owing to the increased stiffness, as demonstrated in Figs. 2 to 5. The table also demonstrates the limit of the core+moment frame system to meet design drift limit. Since the core+moment frame system needs to have extremely stiff core to resist lateral forces, an additional lateral load resisting system such as outrigger system and braced tube system is necessary.

**Table 2.** Steel Tonnage used in Baseline Model and Emboss Tower (in Ton)

| Structural Components/Tower Systems | Baseline Model | Emboss Tower | Δ Between Systems |
|---|---|---|---|
| Perimeter Frame | 8153 | 8789 | +636 (+7%) |
| Core Frame | 16621 | 5817 | -10804 (-65%) |
| Horizontal Members | 6037 | 5168 | -869 (-14%) |
| Total Steel Tonnage | 30811 | 19774 | -11037 (-35%) |

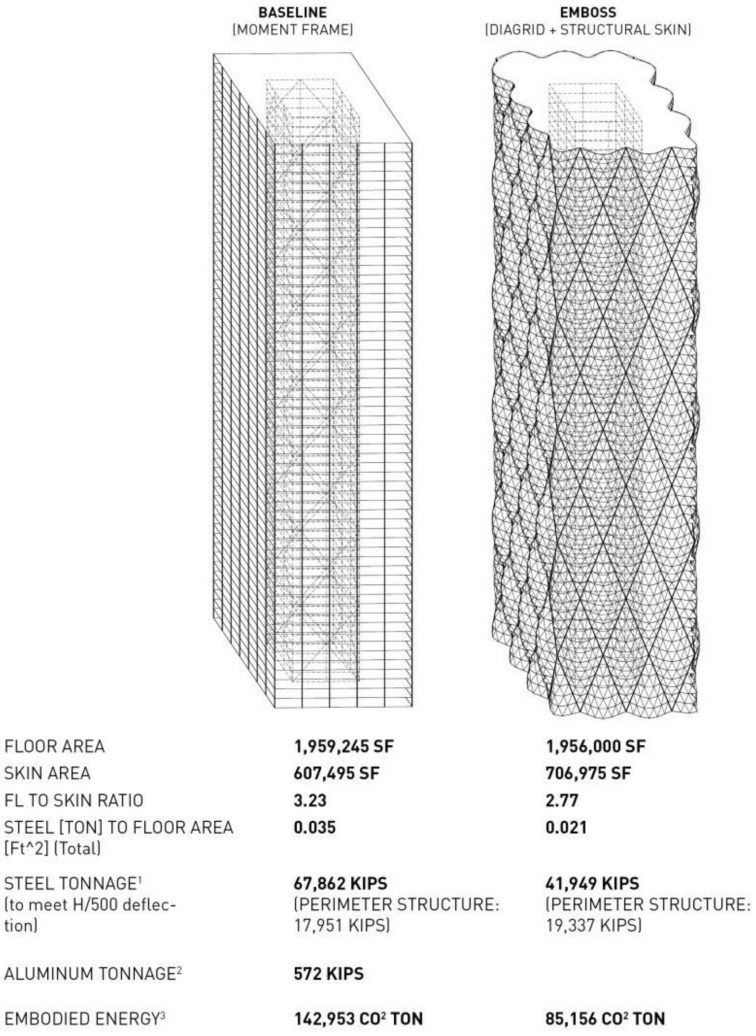



**Figure 13.** Schematic Embodied Energy Comparison.

Embodied energy is calculated from values obtained from the Circular Ecology Database, Inventory of Carbon and Energy (ICE) database. Fig. 13 illustrates the embodied energy comparison between the base and embossed models. In this comparison aluminium tonnage is estimated by the approximation of conventional size of the mullion, 100 mm × 75 mm × 5 mm (thickness), with unit weight 170 lb/cubic ft. The aluminium in the glazing or cassette zone are not included in this schematic comparison. The reduction of the embodied energy due to the replacement of aluminium curtain wall to cassette frames on steel backup mullion is significant, too. According to the standard, the EC (Embodied $CO_2$ and Carbon coefficient) of aluminium is 8.24 $kgCO_2/kg$, while 1.37 $kgCO_2/kg$ for steel.

## 6. Emboss for Efficient Solar Control

The embossed form presents unique conditions for how energy is used and how it affects the interior space. The embossed form increases a typical floor's envelope-to-floor area (average 3416 $m^2$/floor) by approximately 2% over a comparable linear envelope form (3033 $m^2$/floor) bring both benefits and drawbacks for energy efficiency.

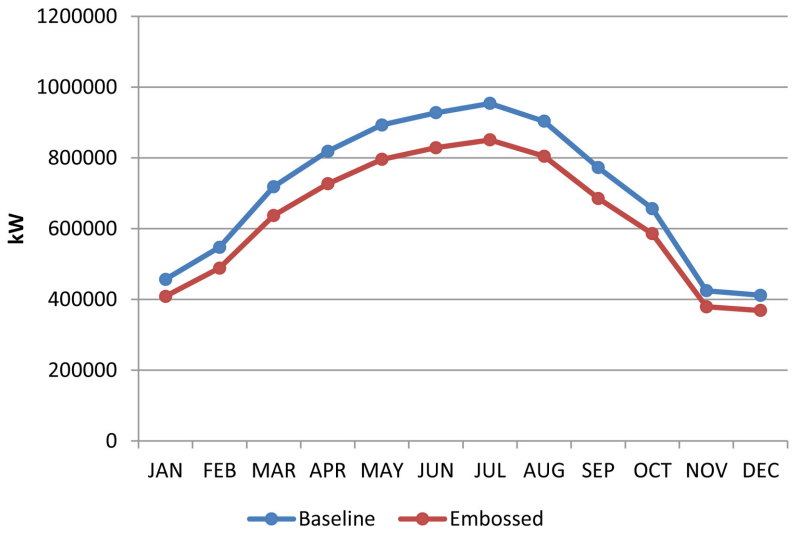



**Figure 14.** Total Transmitted Solar Radiation Energy.

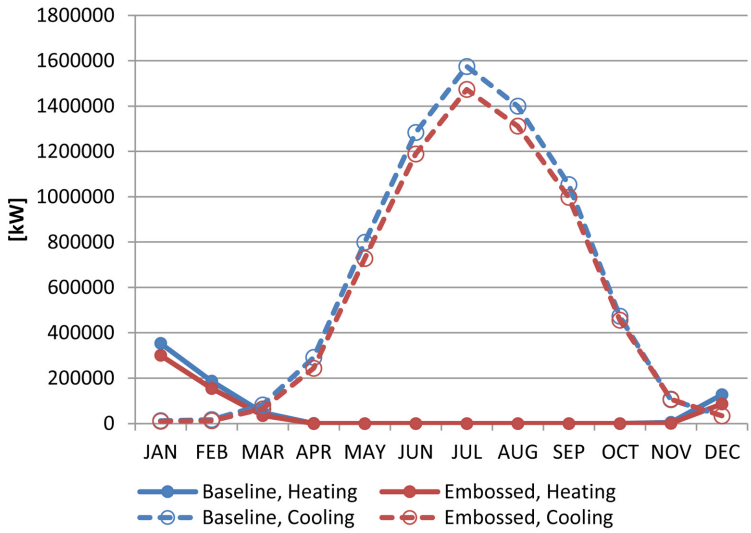



**Figure 15.** Ideal Loads Total Heating and Cooling Energy.

The greater envelope surface area increases the embossed forms exposure to the outdoor weather, similar to a radiator.

Energy performance simulations were run using EnergyPlus v8.6 with both embossed and base models constructed to meet ASHRAE 90.1-2013 (ASHRAE, 2013) minimum compliance levels for climate zone 4A. Modelling assumptions include: ideal air loads, window to wall ratio of 92%, external wall U-factor [0.3634 W/m$^2$·°C] and window U-factor [2.384 W/m$^2$·°C], and default occupancy schedules and loads were obtained from the Department of Energy Commercial prototype building models (U.S. Department of Energy, 2017a). The New York Central Park TMY2 weather file was used (U.S. Department of Energy, 2017b) however; the models were simulated without surrounding context to maintain model simplicity and to ignore shade effects of adjacent buildings.

Simulated energy results considering only lighting, heating and cooling loads show EUI for the embossed form, is 44.3 kWh/m² compared to the baseline form at 45.3 kWh/m². Only 2% difference is seen between the two models (just over 200 MWh). Although this 2% savings in energy use are within a margin of error, how the energy is consumed between the two models is notable; the embossed form uses 5% more electricity for lighting but saves approximately 2% and 4% in cooling and heating loads respectively. Energy use for the embossed tower form is dominated by cooling loads (70%) with 23% of energy used by lighting. What the embossed form appears to be doing, is essentially shifting energy use from cooling

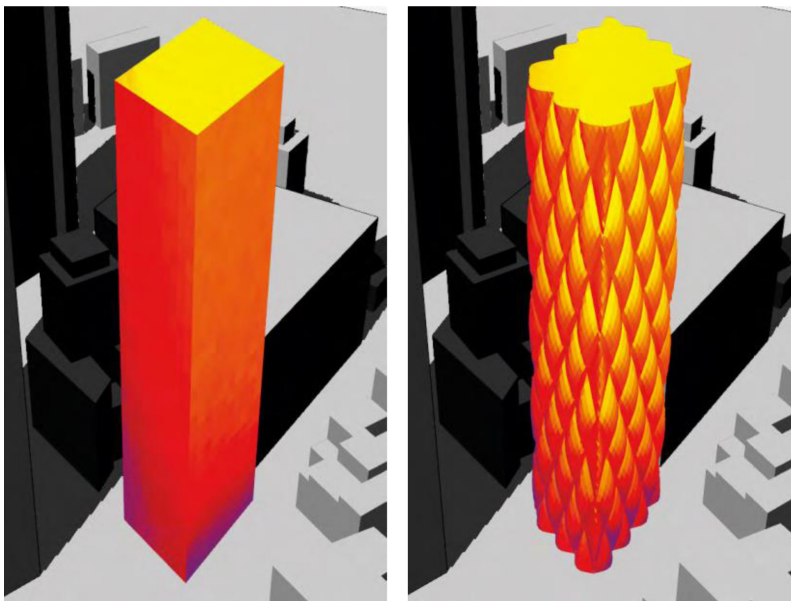


**Figure 16.** Annual solar radiation exposure, on south corner of tower form.

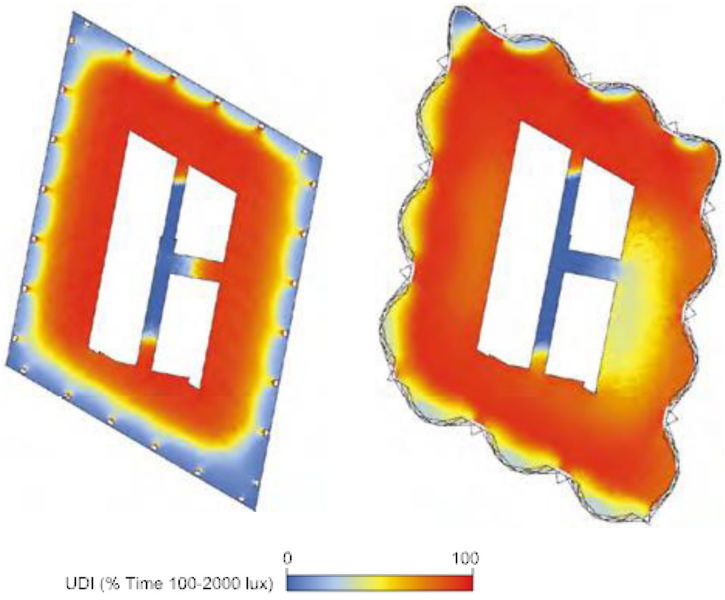



**Figure 17.** Useful Daylight Illuminance (UDI) of a typical floor (embossed average %, rectilinear form average %).

(and heating to a lesser degree) to lighting. This change in energy end use can be explained by how the envelope affects energy exchange by reducing total transmitted solar energy (Fig. 14) which in turn helps reduce the heating and cooling loads (Fig. 15) enough to mitigate the effects of a larger envelope.

With such a dynamic envelope, solar gain can vary significantly between floors and orientation with the embossed form. While a linear envelope form presents a unified angle of incidence and reflection, portions of the embossed envelope will have a more direct angle of incidence while other sub-surfaces will be reflecting direct light, or be partially shaded due to the rippling surface. The resulting annual radiation pattern illustrated in Fig. 16 suggests that architects could specify material and window coatings based on the windows orientation and azimuth angles. This strategy could be continued on the interior where shading strategies and operation could be specified based on these orientation variables as well as user needs (Fig. 19).

In addition to localized solar gain issues, the increased perimeter provides multiple benefits for occupant access

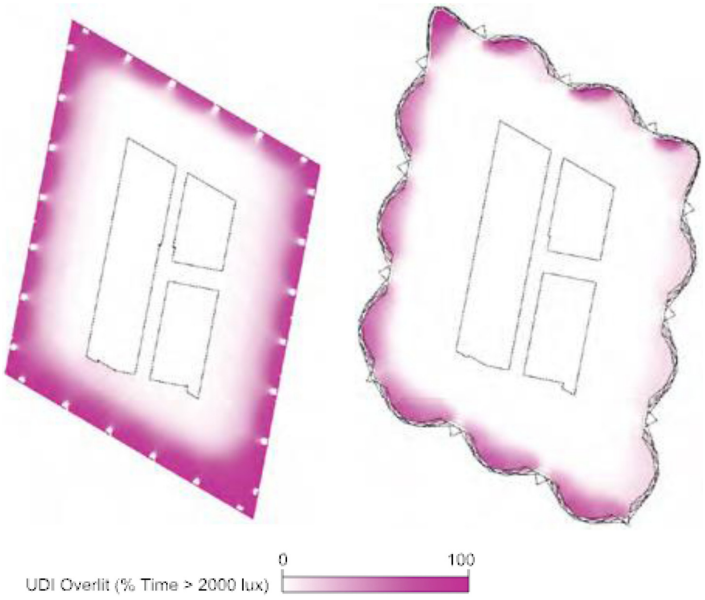



**Figure 18.** Useful Daylight Illuminance (UDI) over lit areas of a typical floor (embossed average %, rectilinear form average %)..

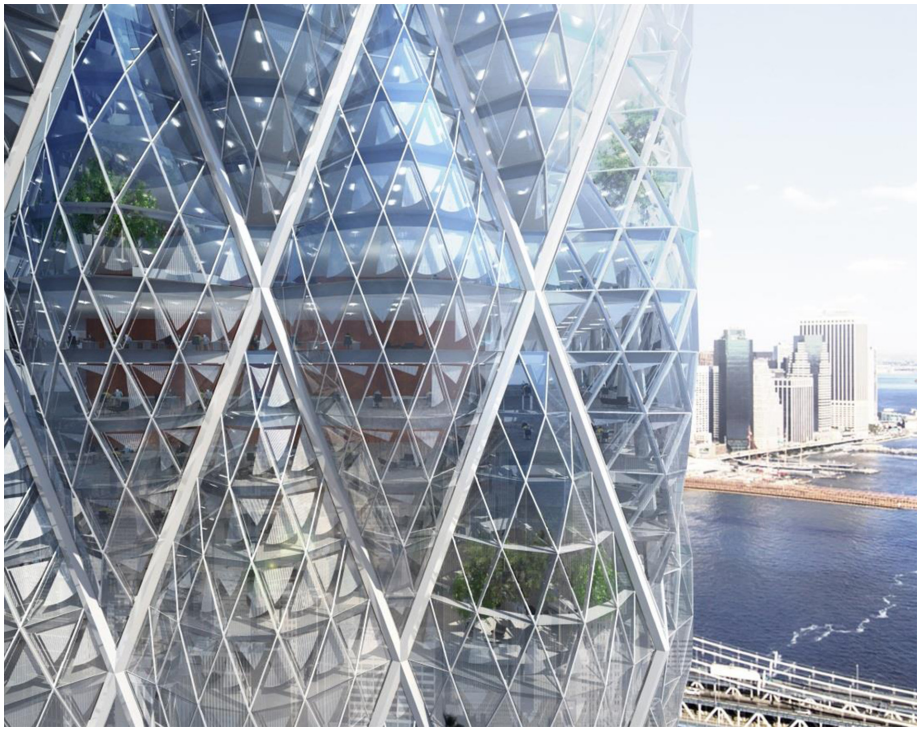


**Figure 19.** Example of localized shading control.

to daylighting. Measuring the contribution of natural light, a typical floor's Useful Daylight Illuminance (UDI), representing the percentage of occupied hours (9:00 to 17:00 hours) when illuminance values are between 100 and 2000 lux, illustrates that more hours of the embossed floor area receives daylight between 100 and 2000 lux (Fig. 17) than a linear form where more hours along the perimeter are in direct sunlight and over lit (Fig. 18). As with solar radiation, solving daylighting issues would enable to architects to select internal shading strategies and window coatings based on local orientation and needs rather than specifying a solution for an entire elevation as would be needed for a rectilinear form.

This same form presenting opportunities for improved

daylighting and mitigating solar radiation, poses another equally challenging set of issues for controlling reflective glare that would impact adjacent buildings. Where a linear building envelope would produce a single angle for reflected light to follow, the embossed form distributes the reflected light in many directions (Fig. 19) requiring more localized solutions for addressing neighbours' concerns. Street level solutions for glare control would differ from mid-level and high-level floors due in part to shading from surrounding context, available direct light, and neighbouring building's needs.

This tower geometry presents a unique design challenge for architects in addressing energy use and occupant comfort. The embossed form would benefit greatly from local solutions for controlling the local indoor environment (Fig. 16), external shading, and glare than a uniform approach derived from each elevations general orientation as would be typical of a linear building envelope. Individual sub-surfaces within the embossed form could be designed with unique glazing and shading qualities that would help mitigate most direct solar radiation and heat loss, while other areas of the envelope could use less costly glazing or utilize different glazing coatings that would provide advantageous qualities to a given orientation and sub-surface azimuth.

## 7. Summary and Conclusions

The Emboss tower geometry presents a unique set of advantages for the future of structural skin. By shaping an underlying diagrid system with an embossed form, an enhanced stiffness to the tower is realized. Structural analysis verifies that the Emboss tower form presents a more efficient structural order by relying on a more efficient structural stiffening effect through embossed sections, and by presenting a surface that disorients wind structure reducing significant aerodynamics loads, resulting in a tower form that is more resource efferent by using less steel. The structural skin supporting the embossed surface eliminates the need for a conventional aluminium curtain wall, which reduces the embodied energy. The embossed skin's convex form produces localized energy control for each sub-surfaces' inclination and orientation which is more efficient than a flat tower. Also, it creates versatile office environments, and presents a unique urban iconography derived from performance of the building skin. However, the conclusions on the effect of enhanced stiffness of the embossed skins were derived from a case study in a model with limited configurations in small number of design parameters. This study needs to be continued further to accommodate various types of design parameters by developing a mathematical model capable of analyzing general types of emboss configurations.

Sustainability in tower design has often been concentrated on membrane performance as feature laden additions to the building due to three fundamental constraints of the typology: repetition of plans, core-heavy moment frames, and prefabricated aluminium curtain walls, which when combined, make prefabricated curtain wall systems a logical and economical choice. With the Embossed design, function of the building envelope has been reimagined with a more holistic role within the building's systems. This design shifts attention from the envelope serving exclusively as a climate barrier and façade to the envelope serving as an integrated system that enhances the building's presence and efficiency through features unique to its form.

## Acknowledgement

The research is an outcome of the collaboration between researchers from University at Buffalo and technical designer and engineer from Skidmore, Owings & Merrill LLP. Chung Yeon Won, AIA, LEED (Former Associate Director at SOM) and Keojin Jin (Designer at SOM) also participated in the proposal.

## References

American Society of Civil Engineers (ASCE), (2010). *Minimum Design Loads for Buildings and Other Structures*, ASCE 7-10. Reston, VA.

American National Standards Institute, Refrigerating and Air-Conditioning Engineers American Society of Heating, and Illuminating Engineering Society of North America (2013). *ANSI/ASHRAE/IES Standard 90.1-2010, Energy Standard for Buildings except Low-Rise Residential Buildings*. Atlanta, GA: American Society of Heating, Refrigerating and Air-Conditioning Engineers, 2013.

Blocken, B., (2014). 50 years of computational wind engineering: past, present and future. *Journal of Wind Engineering and Industrial Aerodynamics*, 129: p. 69-102.

Circular Ecology Database. [Online] Available: http://www.circularecology.com/embodied-energy-and-carbon-footprint-database.html#.WcsvW7KGNgY

Computers and Structures, *SAP2000: Static and Dynamic Finite element Analysis of Structures* (Version 17.2.0). Berkeley, CA

U.S. Department of Energy (2017a). *Commercial Prototype Building Models.* [Online] Available: https://www.energycodes.gov/development/commercial/prototype_models

U.S. Department of Energy (2017b). *Weather Data* [Online] Available: https://energyplus.net/weather

EnergyPlus v8.6. (2017). Department of Energy.

Moon, K., Conner, J., and Fernandez, J. (2007). Diagrid structural systems for tall buildings: Characteristics and methodology for preliminary design. *Struct. Design Tall Spec. Build*. 16, 205-230.

Moon, K. S. (2008) Sustainable structural engineering strategies for tall buildings. *The Structural Design of Tall and Special Buildings* 17, 895-914.

Murakami, S. (1990). Computational Wind Engineering. *Journal of Wind Engineering and Industrial Aerodynamics*, 36, 517-538.

Murakami, S. and Mochida, A. (1999). Past, present and future of CWE: the view from 1999. In: *Wind Engineering into the 21st Century*, p. 91-104.

Neary, J. (2016). Structural Skin. *Proceedings of Facade Tectonics 2016 World Congress, Los Angeles, CA, October 10-11.*

Picon, A. (2014). *Ornament: The politics of architecture and subjectivity.* John Wiley & Sons, p. 129.

Rahimian, A. and Yoram, E. (2006). New York's Hearst Tower. Structure, 25.

Tamura, T., Kawai, H., Kawamoto, S., Nozawa, K., Sakamoto, S., and Ohkuma, T. (1997). Numerical prediction of wind loading on buildings and structures - Activities of AIJ cooperative project on CFD. *Journal of Wind Engineering and Industrial Aerodynamics*, 67, 671-685.